

Continual Contrastive Spoken Language Understanding

Umberto Cappellazzo^{†♦}, Enrico Fini[♡], Muqiao Yang[♣], Daniele Falavigna[♣], Alessio Brutti^{*♣}, and Bhiksha Raj[♣]

[♦]University of Trento


[♡]Independent Researcher

[♣]Carnegie Mellon University

[♣]Fondazione Bruno Kessler

[†] Corresponding author: umberto.cappellazzo@unitn.it

Abstract

Recently, neural networks have shown impressive progress across diverse fields, with speech processing being no exception. However, recent breakthroughs in this area require extensive offline training using large datasets and tremendous computing resources. Unfortunately, these models struggle to retain their previously acquired knowledge when learning new tasks continually. In this paper, we investigate the problem of learning sequence-to-sequence models for spoken language understanding in a class-incremental learning (CIL) setting and we propose COCONUT , a CIL method that relies on the combination of experience replay and contrastive learning. Through a modified version of the standard supervised contrastive loss, COCONUT preserves the learned representations by pulling closer samples from the same class and pushing away the others. Moreover, we leverage a multimodal contrastive loss that helps the model learn more discriminative representations of the new data by aligning audio and text features. We also investigate different contrastive designs to combine the strengths of the contrastive loss with teacher-student architectures used for distillation. Experiments on two established SLU datasets reveal the effectiveness of our proposed approach and significant improvements over the baselines. We also show that COCONUT can be combined with methods that operate on the decoder side, resulting in further metrics improvements.

1 Introduction

With the rapid progress of intelligent voice-enabled personal assistants, the significance of Spoken Language Understanding (SLU) has gained substantial recognition in recent years (Arora et al., 2022; Qin et al., 2021). Conventional SLU models deploy a

cascaded pipeline of an automatic speech recognition (ASR) system followed by a natural language understanding (NLU) module (Mesnil et al., 2014; Horlock and King, 2003). ASR maps the input speech into text representations, and NLU extracts the target intent labels from the intermediate text. Even though these approaches can leverage a vast abundance of ASR and NLU data, they suffer from ASR error propagation. Conversely, end-to-end (E2E) SLU (Agrawal et al., 2022; Lugosch et al., 2019; Saxon et al., 2021) has received more attention in recent research because it uses a single trainable model to map the speech audio directly to the intent labels, bypassing the text transcript and reducing latency and error propagation.

The assumption that the data distribution the model will face after deployment aligns with what it encountered during the training phase is brittle and unrealistic. In fact, real-world scenarios entail evolving streams of data where novel categories (e.g., new vocabulary or intents) emerge sequentially, known as continual learning (CL). Unfortunately, while neural networks thrive in a stationary environment, the situation is reversed in CL, resulting in the “catastrophic forgetting” (CF) of the existing knowledge in favor of fresh new information (McCloskey and Cohen, 1989). Although the majority of CL works have focused on computer vision tasks like image classification (Buzzega et al., 2020; Wang et al., 2022c) and semantic segmentation (Maracani et al., 2021; Yang et al., 2022a), a few works have recently turned their attention towards text (Wang et al., 2023a; Ke et al., 2023) and speech (Cappellazzo et al., 2023a; Diwan et al., 2023), as well as vision-language (Ni et al., 2023; Zhu et al., 2023) and vision-audio (Mo et al., 2023; Pian et al., 2023).

While most SLU works consider offline settings, a thorough study of SLU under a class-incremental learning (CIL) setup still lacks. In CIL, one single model is adapted to a sequence of different tasks as

*This paper has received funding from the European Union’s Horizon research and innovation programme under grant agreement No 101135798, project Meetween (My Personal AI Mediator for Virtual MEETings BetWEEN People)

incremental labels emerge sequentially. Recently, Cappellazzo et al. (2023b) studied the problem of CIL in ASR-SLU, where SLU is carried out in a sequence-to-sequence (seq2seq) fashion, thus computing the intent labels in an auto-regressive way together with the ASR transcriptions. By doing this, the model comprises three blocks: text and audio encoders, and an ASR decoder. While in that work the knowledge distillation (KD) principle applied to the ASR decoder is used, in this paper, we exploit the multi-modal audio-text setting and propose **COCONUT**: **C**Ontinual **C**ontrastive **s**Open **l**aNguage **U**nders**T**anding. COCONUT combines experience replay (ER) and contrastive learning principles. Whereas ER is a well-established approach in CL, whereby a bunch of old training samples are collected into a dedicated rehearsal memory buffer and interleaved with the data from the new task (Rolnick et al., 2019; Bang et al., 2021), only recently has contrastive learning been harnessed to learn representations continually. Both supervised (Cha et al., 2021; Yang et al., 2022a) and self-supervised (Fini et al., 2022; Wang et al., 2022c) contrastive learning have proven useful to lessen the CF issue. Specifically, COCONUT relies on two contrastive learning-based losses that operate on a shared embedding space where the audio and text features are projected.

The first loss coined *Negative-Student Positive-Teacher* (NSPT), is a modified version of the supervised contrastive learning loss that aims to consolidate what the model has learned in the previous tasks. It also exploits KD (Hinton et al., 2015; Li and Hoiem, 2017) to guide the current model (student) to produce representations that resemble the ones obtained with the model from the previous tasks (teacher). *For this reason, this loss is computed only on the rehearsal data (i.e., the anchors).* A key difference between our loss and the standard contrastive one is that the positive samples are computed using the teacher (the positives only come from the rehearsal data), whereas the negatives are computed with the student. In this way, we avoid stale and scattered representations for the new data.

The second loss is inspired by the recent progress in multi-modal representation learning. Considering that for audio-text paired data, audio and text represent the same information but in different ways, it has been shown that aligning their representations results in better performance for various speech-related problems (Zhu et al., 2022; Ye et al., 2022; Manco et al., 2022). Therefore, we propose

a multi-modal (MM) supervised contrastive loss that, *exclusively applied to the current task’s data*, brings audio and text representations belonging to the same class into closer proximity in the shared feature space, resulting in features that are more transferable and resilient to CF. An overview of COCONUT is illustrated in Figure 1.

In summary, our contributions are three-fold: ❶ we introduce COCONUT, a CL method that makes use of two supervised contrastive learning objectives to mitigate CF for seq2seq SLU models. In particular, through our proposed NSPT loss we provide a detailed study of which models (student/teacher) should be used at the numerator/denominator (positives/negatives) of the contrastive loss tailored for class-incremental learning. ❷ We conduct extensive experiments on two popular SLU benchmarks demonstrating that COCONUT achieves consistent improvements over the baselines. We also show that it can be combined with KD applied to the ASR decoder, leading to further improvements. Finally, ❸ we ablate the contribution of each loss and its components, showcasing their pivotal role in COCONUT.

2 Problem Formulation

2.1 ASR-SLU Multi-task Learning

SLU is considered a more difficult task than ASR and NLU since it involves both acoustic and semantic interpretation (Tur and De Mori, 2011). For this reason, it is common practice to include an additional ASR objective such that the SLU labels (in our case the intent labels) and the transcript are generated in an auto-regressive fashion, resulting in a multi-task learning setting (Arora et al., 2022; Peng et al., 2023). By doing this, the text transcript input to the model includes a class intent token that is specific to the actual task.

Let θ be the parameters of a seq2seq ASR model comprising an audio encoder, a text encoder (i.e., embedding layer), and an ASR decoder. Let $\mathbf{x} = [x_0, \dots, x_{U-1}]$ be an audio input sequence of length U , and $\mathbf{y} = [y_{cls}, y_{sep}, y_0, \dots, y_{J-3}]$ be the “extended” input transcript of length J , where with the term “extended” we refer to the original transcript $[y_0, \dots, y_{J-3}]$ augmented with the intent class token y_{cls} and a special separation token y_{sep} . The goal of the ASR model is to find the most likely extended transcript given the input sequence \mathbf{x} :

$$\hat{\mathbf{y}} = \arg \max_{\mathbf{y} \in \mathcal{Y}^*} p(\mathbf{y} | \mathbf{x}; \theta), \quad (1)$$

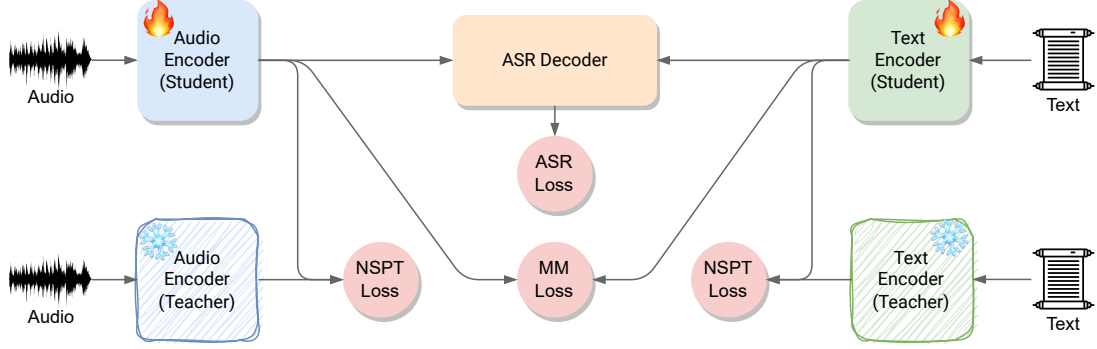



Figure 1: Overview of COCONUT . It uses two contrastive learning-based losses. The NSPT (negative-student positive-teacher) loss is a supervised contrastive distillation loss that preserves the feature representations of the *past* classes for both audio and text samples. The positive and negative samples are computed with the teacher and student model, respectively. The MM (multi-modal) loss aims to align audio and text representations belonging to the same *new* class. COCONUT produces features that are more transferable and resilient to catastrophic forgetting.

where \mathcal{Y}^* is the set of all token sequences. The predicted intent is obtained extracting y_{cls} from $\hat{\mathbf{y}}$.

2.2 Class-Incremental Learning

For our experiments, we consider a CIL setting where we adapt a single model to learn sequentially N tasks corresponding to non-overlapping subsets of classes (in our case *intents*). Put formally, the training dataset is divided into N distinct tasks, $\mathcal{D} = \{\mathcal{D}_0, \dots, \mathcal{D}_{N-1}\}$, based on the intent token y_{cls} , so that one intent is included in one and only one task. The dataset \mathcal{D}_n of task n comprises audio signals \mathcal{X}_n with associated transcriptions \mathcal{Y}_n , i.e. $\mathcal{D}_n = (\mathcal{X}_n, \mathcal{Y}_n)$. The CIL setting is challenging in that the model must be able to distinguish all classes until task n , thus at inference time the task labels are not available (unlike in task-incremental learning) (Hsu et al., 2018).

3 Proposed Approach

3.1 Standard Rehearsal-based Approach

We assume the availability of a rehearsal buffer, \mathcal{M} , in which we can store a few samples for each class encountered in the previous tasks. During the training phase of task n , \mathcal{D}_n , we refer to \mathcal{B} as a mini-batch of samples (\mathbf{x}, \mathbf{y}) , some of which come from the current task and others from the rehearsal memory. To increase the variance of the audio data, we apply SpecAug (Park et al., 2019) to the audio waveform \mathbf{x} (see A.4 for more details). We do not implement any augmentation technique for the transcript \mathbf{y} . We encode each modality separately through a dedicated feature encoder. An audio encoder maps each audio input into a feature vector $\mathbf{h}_A \in \mathbb{R}^{U \times d_A}$, where d_A is the audio hidden size.

Similarly, a text encoder converts each text input into a feature vector $\mathbf{h}_T \in \mathbb{R}^{J \times d_T}$, where d_T is the text hidden size. At this point, if no specific CL losses are used, the ASR decoder generates the output sequence in an auto-regressive fashion, cross-attending on the audio encoder’s representations \mathbf{h}_A . Thus, at task n , we minimize the conventional cross-entropy loss over the current mini-batch \mathcal{B} :

$$\mathcal{L}_{\text{ASR}} = -\frac{1}{|\mathcal{B}|} \sum_{(\mathbf{x}, \mathbf{y}) \in \mathcal{B}} \log(p(\mathbf{y}|\mathbf{x}; \theta)). \quad (2)$$

3.2 COCONUT

Preliminaries. We introduce here some notations for our proposed approach. Since we work with audio and text sequences, we need to aggregate the features we obtain with the encoders before computing the contrastive loss. For the audio component \mathbf{h}_A we apply a mean operation over its sequence length, whereas for text we only select the feature related to the intent token. Then, as is common practice in contrastive learning (Radford et al., 2021; Chen et al., 2020), the resulting embeddings go through two separate linear projection layers that map them into a shared embedding space. At inference time, the projection layers are discarded. Therefore, we get the projected embeddings \mathbf{a} and \mathbf{t} in the following way:

$$\mathbf{a} = g_A(\text{avg}(\mathbf{h}_A)), \quad \mathbf{t} = g_T(\text{cls}(\mathbf{h}_T)), \quad (3)$$

where $\text{cls}(\cdot)$ is a function that extracts the feature associated with the class token, $g_A(\cdot)$ and $g_T(\cdot)$ are the projection layers, $\mathbf{a} \in \mathbb{R}^{d_S}$ and $\mathbf{t} \in \mathbb{R}^{d_S}$, where d_S is the dimension of the shared space.

Furthermore, we introduce some notations for the indices of samples coming from the current

mini-batch \mathcal{B} . Let \mathcal{I}_c and \mathcal{I}_r represent the set of indices of the *new task* samples and the indices of the samples from the rehearsal memory (*old task* samples) in \mathcal{B} , respectively. Also, let $\mathcal{I} = \mathcal{I}_c \cup \mathcal{I}_r$, and we define $\mathcal{P}(k)$ as the set of indices of positive samples (i.e., samples with the same intent token).

The objective of a standard supervised contrastive loss (SCL) (Khosla et al., 2020) is to push the representations of samples with different classes (negative pairs) farther apart while clustering representation of samples with the same class (positive pairs) closely together. Suppose that we get from the projection layers a generic representation \mathbf{z}_i^D for the i -th element in the batch, where $\mathbf{z} = \{\mathbf{a}, \mathbf{t}\}$ and the superscript D denotes whether the representation is computed with the teacher or student model. A generic formulation of the SCL loss takes the following form:

$$\mathcal{L}_{\text{SCL}} = \sum_{k \in \mathcal{I}} \frac{-1}{|\mathcal{P}(k)|} \sum_{p \in \mathcal{P}(k)} \log \frac{\exp(\mathbf{z}_k^D \cdot \mathbf{z}_p^D / \tau)}{\sum_{i \in \mathcal{I}} \exp(\mathbf{z}_k^D \cdot \mathbf{z}_i^D / \tau)}, \quad (4)$$

$\tau \in \mathbb{R}^+$ is a fixed temperature scaling parameter.

Supervised Contrastive Distillation Loss (NSPT). This loss combines the benefits of KD with those of contrastive learning (Tian et al., 2020; Sun et al., 2020). We recall that KD-based methods are very popular in CL and they exploit this paradigm to penalize changes to the model’s intermediate or final outputs by fostering the pass of the knowledge accrued in the teacher model onto the student (Rebuffi et al., 2017; Douillard et al., 2020; Cappellazzo et al., 2023a). Commonly, we denote with *teacher* the model trained in the previous task, and with *student* that trained in the current task. Therefore, since the teacher conveys information about the previous classes, we would like to use it as a guide for the student through a KD objective. In this way, the loss encourages the student to produce audio and text embeddings consistent with those obtained by the teacher. For this reason, only the rehearsal samples are involved in this process as the teacher had no chance to see the current data. Additionally, we want to pull closer embeddings sharing the same intent class (i.e. the positives), while we push away the others (i.e. the negatives, whose class is different). This is obtained via a modified version of the standard supervised contrastive loss tailored for our setting. In fact, a standard one would use the teacher to compute both the positives and the negatives (Khosla et al., 2020). However, since the teacher is frozen

and it is pointless to compute the representations of the samples from the current task using the teacher, we propose to use the student for computing the representations of the negatives. A small fraction of negatives come from the rehearsal buffer, and we also compute them using the student. We show in section 4.3 that using the teacher deteriorates the performance. Therefore, our contrastive distillation loss computes the embeddings of the anchor and its corresponding negatives using the student, while the positives come from the teacher (we call this loss *Negative-Student Positive-Teacher*, NSPT). On the contrary, for the standard contrastive loss both the positives and negatives are computed with the teacher (we call it *Negative-Teacher Positive-Teacher*, NTPT). Figure 2 illustrates visually how the NTPT and NSPT work in the shared embedding space. The NSPT loss is computed for both audio and text embeddings, leading to two components, one for each modality, as follows:

$$\mathcal{L}_{\text{NSPT}} = \sum_{k \in \mathcal{I}_r} \frac{-1}{|\mathcal{P}(k)|} \sum_{p \in \mathcal{P}(k)} \left[\underbrace{\log \frac{\exp(\mathbf{a}_k^n \cdot \mathbf{a}_p^{n-1} / \tau)}{\sum_{i \in \mathcal{I}} \exp(\mathbf{a}_k^n \cdot \mathbf{a}_i^n / \tau)}}_{\mathcal{L}_A} + \underbrace{\log \frac{\exp(\mathbf{t}_k^n \cdot \mathbf{t}_p^{n-1} / \tau)}{\sum_{i \in \mathcal{I}} \exp(\mathbf{t}_k^n \cdot \mathbf{t}_i^n / \tau)}}_{\mathcal{L}_T} \right], \quad (5)$$

where n and $n - 1$ denote whether the representation is obtained with the student or teacher, and \mathcal{L}_A and \mathcal{L}_T represent the audio and text contributions, respectively. We empirically validate that the intuition of the NSPT loss is beneficial in section 4.3.

Supervised Multi-Modal Contrastive Loss.

This loss is introduced for two reasons. First of all, since during the first task (no CL) the NSPT loss is not computed (i.e., we do not have a teacher yet), this means that the projector layers of the model are not trained. This would be a problem from the second task onwards in that the student would distill the knowledge from the teacher with randomly initialized projectors. Second, we want to exploit the multi-modal nature of our SLU CIL setting. Consequently, we introduce a multi-modal (MM) loss that aims to align audio and text representations belonging to the same new class, and thus training the projectors of the model from the very beginning. This alignment is achieved via a supervised multi-modal (i.e., audio-text) contrastive learning objective where feature representations of samples sharing the same intent token are attracted while the others are pushed away. Similar to (Kwon et al.,

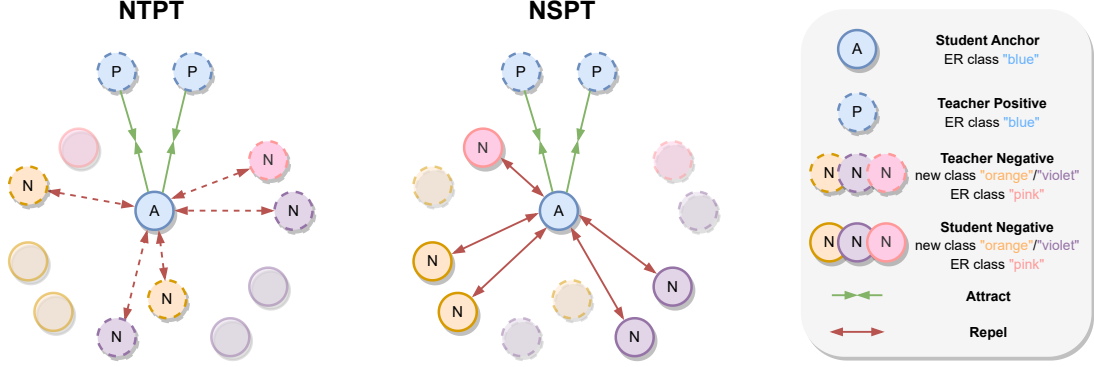


Figure 2: Illustration of the NTPT loss and our proposed NSPT loss. Given an anchor sample from the current mini-batch, the NTPT loss computes the negatives and positives using the teacher model (dashed circles). Instead, the NSPT loss computes the positives with the teacher while the negatives are computed with the student model (solid circles). If the features obtained with the teacher are scattered and static (the teacher is frozen), those obtained with the student are more clustered and can be learned during the current task. Best viewed in color.

2023), we use the [CLS] text token (y_{cls}) for performing the multi-modal alignment. Furthermore, following (Cha et al., 2021), we always treat the rehearsal samples as negatives, preventing them from being anchors during the learning process. This design choice is buttressed by two motivations: **1)** rehearsal data have been learned by the previous model already and are preserved via the NSPT loss, and **2)** we encourage the model to produce clusters for the new data that are separated from those of the rehearsal data. The MM loss is defined as:

$$\mathcal{L}_{MM} = \sum_{k \in \mathcal{I}_c} \frac{-1}{|\mathcal{P}(k)|} \sum_{p \in \mathcal{P}(k)} \left[\log \frac{\exp(\mathbf{a}_k^n \cdot \mathbf{t}_p^n / \tau)}{\sum_{i \in \mathcal{I}} \exp(\mathbf{a}_k^n \cdot \mathbf{t}_i^n / \tau)} + \log \frac{\exp(\mathbf{t}_k^n \cdot \mathbf{a}_p^n / \tau)}{\sum_{i \in \mathcal{I}} \exp(\mathbf{t}_k^n \cdot \mathbf{a}_i^n / \tau)} \right]. \quad (6)$$

The first term of the internal loss is the audio-to-text component, whereas the second is the text-to-audio component (Zhang et al., 2022). The presence of both directions ($A \rightarrow T$ and $T \rightarrow A$) makes the MM loss symmetric. All in all, COCONUT minimizes the following loss:

$$\mathcal{L} = \mathcal{L}_{ASR} + \lambda_{MM} \mathcal{L}_{MM} + \lambda_{NSPT} \mathcal{L}_{NSPT}, \quad (7)$$

where lambdas are loss-specific weights. Note that during the first task \mathcal{L}_{NSPT} is not computed.

4 Experiments

4.1 Experimental Setup and Implementation Details

Datasets and CIL setting. We evaluate COCONUT on two SLU datasets: the Fluent Speech Commands (FSC) (Lugosch et al., 2019) and the

Spoken Language Understanding Resource Package (SLURP) (Bastianelli et al., 2020). FSC includes 30,043 English utterances, recorded at 16 kHz, resulting in 31 intent classes in total. The SLURP dataset comprises around 56 hours of audio of people interacting with a home assistant (*slurp_real*), with the addition of 43.5 hours of synthetic data (*slurp_synth*). It is considered the most challenging SLU dataset due to its lexical complexity. Each utterance is annotated with 3 semantics: scenario, action, and entity. The pair (scenario, action) defines an intent. Overall, there are 18 scenarios and 69 intents. For our experiments, we only perform intent classification. Following (Cappellazzo et al., 2023b), we use the scenario labels as splitting criterion to define the CIL setting (we refer to A.3 for more details on this). We experiment on two configurations: 1) the datasets are partitioned into 3 tasks, each task comprising 6 scenarios for SLURP (denoted as SLURP-3), and 10 intents for FSC (FSC-3); 2) a more challenging configuration with 6 tasks, each task including 3 scenarios for SLURP (SLURP-6), and 5 intents for FSC (FSC-6).

Implementation Details. For both datasets, the text encoder is a standard text embedding layer with size 768. For the audio encoder, we use a Wav2vec 2.0 base model (Baevski et al., 2020) pre-trained and fine-tuned on 960 hours of Librispeech for SLURP ($\sim 94.3M$ parameters), while we use DistilHuBERT base (Chang et al., 2022) for FSC ($\sim 23.5M$ parameters). Both encoders have hidden sizes of 768. Since FSC is a less challenging dataset than SLURP, we found that a smaller pre-trained encoder is sufficient to achieve state-of-the-

Table 1: Results in terms of Average Accuracy (\uparrow), Last Accuracy (\uparrow), and Average WER (\downarrow) for different strategies on FSC and SLURP datasets. All CL methods exploit a buffer whose size is 1% of the training dataset. **Bold** and underline numbers denote the best and second best method for a specific setting and metric, respectively. We show in the last row that COCONUT and S-KD can be used together, leading to the best results. For simplicity, the values of the last row are not in bold even though attain the best results.

Setting \rightarrow	FSC-3			FSC-6			SLURP-3			SLURP-6		
Metric \rightarrow	Avg	Last	Avg	Avg	Last	Avg	Avg	Last	Avg	Avg	Last	Avg
Method \downarrow	Acc	Acc	WER	Acc	Acc	WER	Acc	Acc	WER	Acc	Acc	WER
Offline	99.28	-	0.48	99.28	-	0.48	84.41	-	17.65	84.41	-	17.65
Fine-tuning	49.13	17.61	36.37	29.92	7.59	54.66	46.65	18.42	28.32	31.90	10.57	34.79
ER rand	79.17	69.81	15.87	68.61	63.71	24.04	71.44	61.88	21.25	66.57	58.22	24.50
ER iCaRL	82.04	74.00	13.45	69.76	64.12	23.22	71.94	63.22	<u>21.06</u>	68.08	62.29	26.05
T-KD	82.11	75.43	12.95	69.08	64.73	23.82	72.44	62.43	21.19	66.95	60.47	24.26
A-KD	<u>84.79</u>	<u>78.12</u>	<u>11.54</u>	73.54	67.05	<u>20.36</u>	72.10	63.84	20.67	68.52	62.51	<u>24.29</u>
S-KD	84.29	75.31	12.39	<u>73.65</u>	<u>67.71</u>	21.27	74.28	65.95	21.26	69.91	<u>63.22</u>	24.26
COCONUT	86.39	80.21	11.08	77.09	73.80	19.05	<u>72.75</u>	<u>64.62</u>	21.25	70.17	63.66	<u>24.29</u>
<u>COCONUT+S-KD</u>	87.64	80.45	10.49	77.57	74.01	18.47	75.58	67.39	20.61	71.91	65.41	24.16

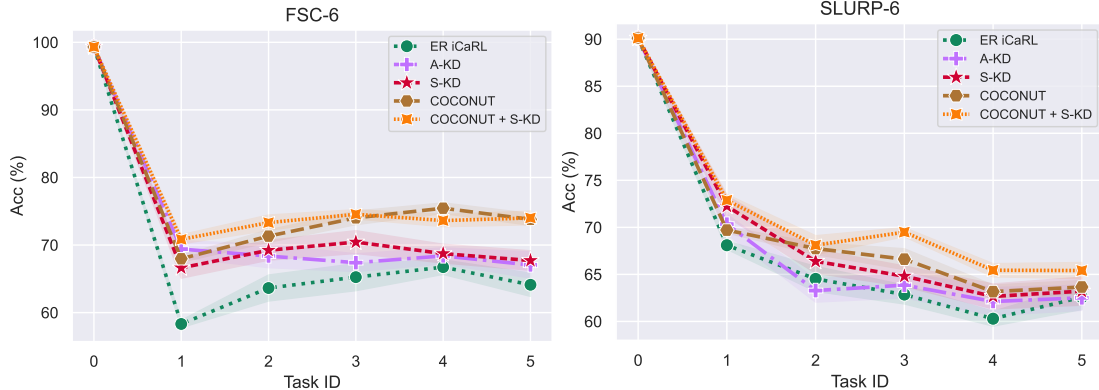


Figure 3: *Left*: the trend of the intent accuracy on the observed tasks for the FSC-6 setting. *Right*: the trend of the intent accuracy on the observed tasks for SLURP-6.

art results. Moreover, experimenting with diverse architectures helps evaluate the generalizability of our proposed method. As in (Radford et al., 2021), we employ linear projection layers to map from each encoder’s representation to the audio-text embedding space, whose dimension is 512. The ASR decoder is transformer-based with 6 layers, hidden size equal to 768, 8 attention heads, and the dimension of the feedforward layers is 2048. We set the temperature τ to 0.1 for both NSPT and MM loss (please refer to 4.4 for a detailed analysis).

For the tokenization we apply Byte-Pair Encoding (BPE) (Sennrich et al., 2016) for SLURP, with a vocabulary size of 1000 and BPE dropout equal to 0.1, whereas for FSC, given the limited number of unique words, we use word tokenization, resulting in 139 tokens. BPE automatically assigns to each intent a dedicated token, whereas for FSC we

manually add the intent tokens. We refer the reader to A.2 for an exhaustive description of the hyperparameters. Regarding the weight coefficients, we set λ_{MM} to 0.1, and similarly to (Douillard et al., 2022; Wu et al., 2019) we set λ_{NSPT} to $\frac{L_p}{L_p+L_n}$, where L_p and L_n count the number of past and new classes.

Baselines. Apart from the standard **offline** (1 task, no continual) and **fine-tuning** (no CL strategies) baselines, we compare COCONUT against standard **experience replay** (ER) methods with *random* and *iCaRL* (Rebuffi et al., 2017) sampling strategies. We note that ER is already a strong baseline for FSC and SLURP. We also point out that adapting standard CL strategies to our setting is not trivial as they are usually proposed for classification tasks and not for auto-regressive tasks. Plus, we report two methods proposed in (Cappellazzo et al., 2023b) that combine rehearsal and KD prin-

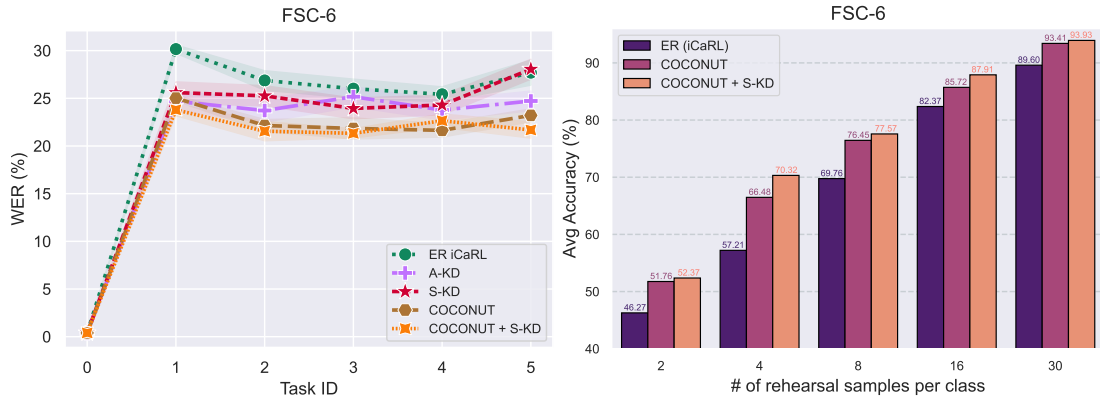


Figure 4: *Left*: the trend of the WER on the observed tasks for the FSC-6 setting. *Right*: the accuracy of COCONUT and other methods as a function of the memory size.

principles: audio-KD (**A-KD**) that applies the KD on the audio features of the rehearsal samples, and seq-KD (**S-KD**) that, at the end of the current task, stores the text transcriptions computed with beam search only for the rehearsal samples and use them as pseudo-transcriptions for the next task. This method operates on the ASR decoder. For the sake of completeness, we also report text-KD (**T-KD**), the text counterpart of the A-KD.

Metrics. Following (Douillard et al., 2022), we report the results in terms of the *Avg Acc*, which is the average of the intent accuracies after each training task, and the *Last Acc*, which is the intent accuracy after the last task. We also report the *Avg WER*, the average of the Word Error Rate (WER) of the extended transcription after each task.

4.2 Main Results

In the first two rows of Table 1, we include the upper and lower bounds represented by the offline learning (which is in line with the state-of-the-art) and fine-tuning approaches. For the fine-tuning approach, we can notice how CF deteriorates the knowledge of the prior classes. We then include ER baselines with buffer capacity equal to 1% of the dataset size. From these results we can see that ER-based methods achieve good results for all metrics and configurations, confirming themselves as solid baselines. For FSC, COCONUT outperforms the other baselines by a significant margin, in terms of both accuracy and WER. Its combination with the S-KD leads to additional improvements (last row).

If we turn our focus to SLURP we see that, for the setting with 3 tasks, S-KD turns out to be the best approach in terms of intent accuracy, followed by COCONUT. For the WER, all the methods achieve similar performance and do not provide

significant enhancements. We speculate that, as only some words are task-specific while the others are spread across multiple tasks, the text modality is less affected by CF. It is also compelling to note that the A-KD always achieves better performance than T-KD, a trend that will also be observed for the NSPT loss in the ablation studies. For SLURP-6, COCONUT slightly surpasses S-KD in terms of accuracy, and performs on par with the others for the WER metric. This indicates that COCONUT scales properly with the number of tasks. Additionally, we point out that, for SLURP, COCONUT provides less noticeable improvements than FSC. This can be attributable to the higher complexity of the dataset due to its larger dictionary and to the larger number of intents with respect to FSC (69 vs. 31). Finally, similar to FSC, the combination of COCONUT with S-KD attains the best results, confirming that fighting CF both at the encoders and ASR decoder is an effective solution.

In Fig. 3 we illustrate the trend of the intent accuracy after each task for FSC-6 and SLURP-6. For FSC-6, COCONUT outperforms the other baselines by a large margin after each task. For SLURP-6, COCONUT has a similar trend as S-KD, and their combination leads to a noteworthy boost in performance. On the left part of Fig. 4 we also show the trend of the WER task by task.

4.3 Ablation Study

Is COCONUT effective when we vary the buffer memory size? On the right side of Fig. 4, we study the trend of COCONUT for different quantities of rehearsal samples per class. Note that 8 samples per class is equivalent to a buffer capacity of 1% of the entire training dataset. The maximum gain provided by COCONUT with respect to the

Table 2: Ablation on the use of NSPT and NTPT losses.

Dataset →	FSC-6		SLURP-6	
	Avg Acc	Last Acc	Avg Acc	Last Acc
ER iCaRL	69.76	64.12	68.08	62.29
MM	71.12	67.76	68.78	62.94
MM + NTPT	74.05	67.61	68.91	62.57
MM + NSPT-AA	76.30	72.34	69.74	62.54
MM + NSPT-AN	66.37	63.89	64.72	56.84
MM + NSPT	77.09	73.80	70.17	63.66

ER baseline is reached for 4 and 8 samples per class (9.27 and 6.69, respectively), while for the extreme cases of 2 and 30 samples, the gap is reduced. This is explained by the fact that when few samples are stored for each class, the effect of the NSPT loss is highly reduced given its reliance on the rehearsal data, whilst in the opposite case the abundance of rehearsal data makes the ER baseline already strong, thereby improving it becomes more challenging. Regarding the latter case we note that when we increase the buffer memory size, we implicitly move toward the offline setting (the upper bound), which is not the objective of this paper.

Ablation on the NSPT Loss. In Table 2 we evaluate the difference in performance between the standard NTPT loss and our proposed NSPT loss and some of its variants. Specifically, we study two design properties: **1)** which samples should be used as anchors? **2)** Should the rehearsal negatives be computed using the teacher model rather than the student, unlike the negatives coming from the new task? Regarding point **(1)**, we study the case where the anchor samples are both the rehearsal data (our proposed design) *and* the new data. This means that in the outer sum of Equation 5 the samples are picked from \mathcal{I} . Note that this design choice requires to compute the loss for all samples in the dataset, thus incurring an appreciable increase in the computational cost. We denote this variant where we Ablate the Anchor design as NSPT-AA. As for the second point, we compute the negatives coming from the rehearsal memory using the teacher (the teacher has seen those classes in the previous tasks), whereas the samples from the current task are computed with the student model. The denominators of Equation 5 become (we use \mathbf{z} to refer to both \mathbf{a} and \mathbf{t}): $\sum_{i \in \mathcal{I}_c} \exp(\mathbf{z}_k^n \cdot \mathbf{z}_i^n / \tau) + \sum_{h \in \mathcal{I}_r} \exp(\mathbf{z}_k^n \cdot \mathbf{z}_h^{n-1} / \tau)$. We call it NSPT-AN (Ablate Negatives).

Table 3: Ablation study of the MM (upper part) and NSPT (bottom part) components. **CLS**: whether only the intent class token is used; **Anchor**: whether ER data are excluded from the anchors. $\mathcal{L}_A/\mathcal{L}_T$: whether the audio/text component of NSPT loss is used.

CLS	Anchor	\mathcal{L}_A	\mathcal{L}_T	Avg Acc
				70.10
✓				70.49
	✓			71.09
✓	✓			71.12
✓	✓	✓		76.84
✓	✓		✓	73.11
✓	✓	✓	✓	77.09

Looking at Table 2, we see that for FSC-6, the use of our proposed NSPT loss gives a considerable improvement over the NTPT loss in terms of all three considered metrics. For SLURP-6, the trend is maintained, and now the NTPT even brings a small deterioration over the MM baseline in terms of Last Acc. Also, the MM loss alone contributes positively over the ER baseline for both settings. We recall that it is not possible to study the individual contribution of the NSPT loss because, without the MM loss, the teacher projectors are randomly initialized during the second task (see section 3.2). Furthermore, we observe that the design choices of **(1)** and **(2)** are crucial to obtaining superior performance. Regarding the NSPT-AA loss, the model is less sensitive to this design choice. However, note that this loss is more expensive as it requires extra computational cost owing to the use of all samples in a mini-batch for its computation, thus making it less appealing than our proposed NSPT loss. Instead, the use of the NSPT-AN yields a severe degradation in the performance. We suspect that this happens because mixing the teacher and student at the denominators makes the learning process more complex as feature representations of different models interact, inducing more interference and thus leading the model to make more mistakes.

Ablation on the MM Loss. Finally, in Table 3 we study the design properties of the MM loss on FSC-6, and with its best configuration, we determine the individual contribution of the audio and text components to the NSPT loss. For the MM loss, we see that using the intent token and preventing the ER data from being anchors brings additional improvements. For the NSPT loss, as

Table 4: Ablation study of the temperature τ for the MM loss. We experiment on FSC-6 by setting τ beforehand and making it a learnable hyperparameter as is common practice in offline settings (Radford et al., 2021). The light-blue row corresponds to the value we used for our experiments.


Metric \rightarrow Temp. (τ) \downarrow	Avg Acc	Last Acc	Avg WER
0.07	71.06	64.75	22.07
0.1	71.12	67.76	22.88
0.2	71.01	62.35	22.78
Learnable	69.05	66.33	24.57

was evident for the A-KD and T-KD, with the former giving better results, here we also discover that the audio component is predominant. Plus, the concurrent use of both components brings a moderate increase in accuracy, and this is due to the alignment between audio and text via the MM loss.

4.4 On the Impact of the Temperature Parameter

In this section we analyze the role of the temperature parameter in the CIL process for the MM loss (see Equation 6) on the FSC-6 setting. We first try to set the value beforehand (0.07, 0.1, 0.2), and then we make the temperature a learnable hyperparameter (initial value is 0.07). Results are reported in Table 4. We can observe that $\tau = 0.1$ is the best configuration for the accuracy metric. Note that, however, the model does not seem very sensitive to the temperature for the Avg Acc, whereas the Last Acc is more influenced. Since the Avg Acc does not change much across the three configurations, yet the Last Acc sways much more, this means that for $\tau = 0.1$ the model struggles more during the initial tasks, but it performs better towards the end of the learning process. On the other hand, learning τ task by task does not seem to be the right choice as the Avg Acc and WER metrics deteriorate with respect to the other three configurations where it is fixed. In fact, we observed that during the first tasks, the model is learning the optimal value for τ until it finds it (this value approximately lies in the range 0.134–0.142). This initial transitional phase penalizes the accuracy of the first tasks, which in turn leads to a deterioration in the Avg Acc metric.

5 Conclusion

In this work, we study the problem of E2E SLU using a seq-2-seq model for class-incremental learning. In order to mitigate catastrophic forgetting we propose COCONUT , a CL approach that exploits experience replay and contrastive learning paradigms. On the one hand, it preserves the previously learned feature representations via an ad-hoc supervised contrastive distillation loss, on the other it contributes to aligning audio and text representations, thus resulting in more transferable and robust to catastrophic forgetting representations. We show that COCONUT outperforms the other baselines and that synergizes with other KD techniques operating on the decoder side. We finally dissect the design choices of COCONUT through specific ablation studies, showcasing that each component is pivotal to attain the best results.

6 Limitations

Our work comes with some limitations. First of all, the number of suitable SLU datasets for CIL settings is limited since few datasets provide enough intent classes. Then, we could not use batches larger than 32 owing to computational limitations, and it is known that contrastive learning benefits from larger batches. Finally, as pointed out in the paper, almost all CIL methods are proposed for classification tasks, so their adaptation to our setting is not trivial. For this reason, we focused more on past baselines tailored for our setting, as well as rehearsal approaches that confirm themselves as strong approaches while being simple. Finally, we do not see any potential risks linked to our work.

References

- Bhuvan Agrawal, Markus Müller, Samridhi Choudhary, Martin Radfar, Athanasios Mouchtaris, Ross McGowan, Nathan Susanj, and Siegfried Kunzmann. 2022. Tie your embeddings down: Cross-modal latent spaces for end-to-end spoken language understanding. In *IEEE International Conference on Acoustics, Speech and Signal Processing (ICASSP)*, pages 7157–7161. IEEE.
- Rahaf Aljundi, Punarjay Chakravarty, and Tinne Tuytelaars. 2017. Expert gate: Lifelong learning with a network of experts. In *Proceedings of the IEEE Conference on Computer Vision and Pattern Recognition*, pages 3366–3375.
- Siddhant Arora, Siddharth Dalmia, Pavel Denisov, Xunkai Chang, Yushi Ueda, Yifan Peng, Yuekai Zhang,

- Sujay Kumar, Karthik Ganesan, Brian Yan, et al. 2022. Espnet-slu: Advancing spoken language understanding through espnet. In *IEEE International Conference on Acoustics, Speech and Signal Processing (ICASSP)*, pages 7167–7171. IEEE.
- Alexei Baevski, Yuhao Zhou, Abdelrahman Mohamed, and Michael Auli. 2020. wav2vec 2.0: A framework for self-supervised learning of speech representations. *Advances in neural information processing systems*, 33:12449–12460.
- Jihwan Bang, Heesu Kim, YoungJoon Yoo, Jung-Woo Ha, and Jonghyun Choi. 2021. Rainbow memory: Continual learning with a memory of diverse samples. In *Proceedings of the IEEE/CVF Conference on Computer Vision and Pattern Recognition*, pages 8218–8227.
- Emanuele Bastianelli, Andrea Vanzo, Pawel Swietojanski, and Verena Rieser. 2020. [SLURP: A spoken language understanding resource package](#). In *Proceedings of the 2020 Conference on Empirical Methods in Natural Language Processing (EMNLP)*, pages 7252–7262, Online. Association for Computational Linguistics.
- Pietro Buzzega, Matteo Boschini, Angelo Porrello, Davide Abati, and Simone Calderara. 2020. Dark experience for general continual learning: a strong, simple baseline. *Advances in neural information processing systems*, 33:15920–15930.
- Umberto Cappellazzo, Daniele Falavigna, and Alessio Brutti. 2023a. An investigation of the combination of rehearsal and knowledge distillation in continual learning for spoken language understanding. *Proceedings of Interspeech*.
- Umberto Cappellazzo, Muqiao Yang, Daniele Falavigna, and Alessio Brutti. 2023b. Sequence-level knowledge distillation for class-incremental end-to-end spoken language understanding. *Proceedings of Interspeech*.
- Hyuntak Cha, Jaeho Lee, and Jinwoo Shin. 2021. Co2l: Contrastive continual learning. In *Proceedings of the IEEE/CVF International conference on computer vision*, pages 9516–9525.
- Heng-Jui Chang, Shu-wen Yang, and Hung-yi Lee. 2022. Distilhubert: Speech representation learning by layer-wise distillation of hidden-unit bert. In *IEEE International Conference on Acoustics, Speech and Signal Processing (ICASSP)*, pages 7087–7091. IEEE.
- Arslan Chaudhry, Marc’Aurelio Ranzato, Marcus Rohrbach, and Mohamed Elhoseiny. 2019. Efficient lifelong learning with a-gem. *Proceedings of ICLR*.
- Ting Chen, Simon Kornblith, Mohammad Norouzi, and Geoffrey Hinton. 2020. A simple framework for contrastive learning of visual representations. In *International conference on machine learning*, pages 1597–1607. PMLR.
- Anuj Diwan, Ching-Feng Yeh, Wei-Ning Hsu, Paden Tomasello, Eunsol Choi, David Harwath, and Abdelrahman Mohamed. 2023. Continual learning for on-device speech recognition using disentangled conformers. In *IEEE International Conference on Acoustics, Speech and Signal Processing (ICASSP)*, pages 1–5. IEEE.
- Arthur Douillard, Matthieu Cord, Charles Ollion, Thomas Robert, and Eduardo Valle. 2020. Podnet: Pooled outputs distillation for small-tasks incremental learning. In *Computer vision—ECCV 2020: 16th European conference, Glasgow, UK, August 23–28, 2020, proceedings, part XX 16*, pages 86–102. Springer.
- Arthur Douillard, Alexandre Ramé, Guillaume Couairon, and Matthieu Cord. 2022. Dytox: Transformers for continual learning with dynamic token expansion. In *Proceedings of the IEEE/CVF Conference on Computer Vision and Pattern Recognition*, pages 9285–9295.
- Sayna Ebrahimi, Mohamed Elhoseiny, Trevor Darrell, and Marcus Rohrbach. 2020. Uncertainty-guided continual learning with bayesian neural networks. *Proceedings of ICLR*.
- Enrico Fini, Victor G Turrissi Da Costa, Xavier Alameda-Pineda, Elisa Ricci, Karteek Alahari, and Julien Mairal. 2022. Self-supervised models are continual learners. In *Proceedings of the IEEE/CVF Conference on Computer Vision and Pattern Recognition*, pages 9621–9630.
- Enrico Fini, Stéphane Lathuiliere, Enver Sangineto, Moin Nabi, and Elisa Ricci. 2020. Online continual learning under extreme memory constraints. In *Computer Vision—ECCV 2020: 16th European Conference, Glasgow, UK, August 23–28, 2020, Proceedings, Part XXVIII 16*, pages 720–735. Springer.
- Jie Gui, Tuo Chen, Qiong Cao, Zhenan Sun, Hao Luo, and Dacheng Tao. 2023. A survey of self-supervised learning from multiple perspectives: Algorithms, theory, applications and future trends. *arXiv preprint arXiv:2301.05712*.
- Geoffrey Hinton, Oriol Vinyals, and Jeff Dean. 2015. Distilling the knowledge in a neural network. *arXiv preprint arXiv:1503.02531*.
- James Horlock and Simon King. 2003. [Discriminative methods for improving named entity extraction on speech data](#). In *Proc. 8th European Conference on Speech Communication and Technology (Eurospeech 2003)*, pages 2765–2768.
- Saihui Hou, Xinyu Pan, Chen Change Loy, Zilei Wang, and Dahua Lin. 2018. Lifelong learning via progressive distillation and retrospection. In *Proceedings of the European Conference on Computer Vision (ECCV)*, pages 437–452.
- Yen-Chang Hsu, Yen-Cheng Liu, Anita Ramasamy, and Zsolt Kira. 2018. Re-evaluating continual learning

- scenarios: A categorization and case for strong baselines. *arXiv preprint arXiv:1810.12488*.
- Zixuan Ke, Yijia Shao, Haowei Lin, Tatsuya Konishi, Gyuhak Kim, and Bing Liu. 2023. Continual pre-training of language models. In *The Eleventh International Conference on Learning Representations*.
- Prannay Khosla, Piotr Teterwak, Chen Wang, Aaron Sarna, Yonglong Tian, Phillip Isola, Aaron Maschiot, Ce Liu, and Dilip Krishnan. 2020. Supervised contrastive learning. *Advances in neural information processing systems*, 33:18661–18673.
- James Kirkpatrick, Razvan Pascanu, Neil Rabinowitz, Joel Veness, Guillaume Desjardins, Andrei A Rusu, Kieran Milan, John Quan, Tiago Ramalho, Agnieszka Grabska-Barwinska, et al. 2017. Overcoming catastrophic forgetting in neural networks. *Proceedings of the national academy of sciences*, 114(13):3521–3526.
- Gukyeong Kwon, Zhaowei Cai, Avinash Ravichandran, Erhan Bas, Rahul Bhotika, and Stefano Soatto. 2023. Masked vision and language modeling for multi-modal representation learning. *Proceedings of ICLR*.
- Zhizhong Li and Derek Hoiem. 2017. Learning without forgetting. *IEEE transactions on pattern analysis and machine intelligence*, 40(12):2935–2947.
- Loren Lugosch, Mirco Ravanelli, Patrick Ignoto, Vikrant Singh Tomar, and Yoshua Bengio. 2019. Speech model pre-training for end-to-end spoken language understanding. *Proceedings of Interspeech*.
- Ilaria Manco, Emmanouil Benetos, Elio Quinton, and György Fazekas. 2022. Contrastive audio-language learning for music. *Proceedings of ISMIR*.
- Andrea Maracani, Umberto Michieli, Marco Toldo, and Pietro Zanuttigh. 2021. Recall: Replay-based continual learning in semantic segmentation. In *Proceedings of the IEEE/CVF international conference on computer vision*, pages 7026–7035.
- Michael McCloskey and Neal J Cohen. 1989. Catastrophic interference in connectionist networks: The sequential learning problem. In *Psychology of learning and motivation*, volume 24, pages 109–165. Elsevier.
- Grégoire Mesnil, Yann Dauphin, Kaisheng Yao, Yoshua Bengio, Li Deng, Dilek Hakkani-Tur, Xiaodong He, Larry Heck, Gokhan Tur, Dong Yu, et al. 2014. Using recurrent neural networks for slot filling in spoken language understanding. *IEEE/ACM Transactions on Audio, Speech, and Language Processing*, 23(3):530–539.
- Shentong Mo, Weiguo Pian, and Yapeng Tian. 2023. Class-incremental grouping network for continual audio-visual learning. *Proceedings of ICCV*.
- Zixuan Ni, Longhui Wei, Siliang Tang, Yueting Zhuang, and Qi Tian. 2023. Continual vision-language representation learning with off-diagonal information. *Proceedings of ICML*.
- Aaron van den Oord, Yazhe Li, and Oriol Vinyals. 2018. Representation learning with contrastive predictive coding. *arXiv preprint arXiv:1807.03748*.
- Oleksiy Ostapenko, Pau Rodriguez, Massimo Caccia, and Laurent Charlin. 2021. Continual learning via local module composition. *Advances in Neural Information Processing Systems*, 34:30298–30312.
- Daniel S Park, William Chan, Yu Zhang, Chung-Cheng Chiu, Barret Zoph, Ekin D Cubuk, and Quoc V Le. 2019. SpecAugment: A simple data augmentation method for automatic speech recognition. *arXiv preprint arXiv:1904.08779*.
- Yifan Peng, Siddhant Arora, Yosuke Higuchi, Yushi Ueda, Sujay Kumar, Karthik Ganesan, Siddharth Dalmia, Xuankai Chang, and Shinji Watanabe. 2023. A study on the integration of pre-trained ssl, asr, lm and slu models for spoken language understanding. In *2022 IEEE Spoken Language Technology Workshop (SLT)*, pages 406–413. IEEE.
- Weiguo Pian, Shentong Mo, Yunhui Guo, and Yapeng Tian. 2023. Audio-visual class-incremental learning. *Proceedings of ICCV*.
- Libo Qin, Tianbao Xie, Wanxiang Che, and Ting Liu. 2021. A survey on spoken language understanding: Recent advances and new frontiers. *Proceedings of IJCAI*.
- Alec Radford, Jong Wook Kim, Chris Hallacy, Aditya Ramesh, Gabriel Goh, Sandhini Agarwal, Girish Sastry, Amanda Askell, Pamela Mishkin, Jack Clark, et al. 2021. Learning transferable visual models from natural language supervision. In *International conference on machine learning*, pages 8748–8763. PMLR.
- Mirco Ravanelli, Titouan Parcollet, Peter Plantinga, Aku Rouhe, Samuele Cornell, Loren Lugosch, Cem Subakan, Nauman Dawalatabad, Abdelwahab Heba, Jianyuan Zhong, et al. 2021. Speechbrain: A general-purpose speech toolkit. *arXiv preprint arXiv:2106.04624*.
- Sylvestre-Alvise Rebuffi, Alexander Kolesnikov, Georg Sperl, and Christoph H Lampert. 2017. iCaRL: Incremental classifier and representation learning. In *Proceedings of the IEEE conference on Computer Vision and Pattern Recognition*, pages 2001–2010.
- David Rolnick, Arun Ahuja, Jonathan Schwarz, Timothy Lillicrap, and Gregory Wayne. 2019. Experience replay for continual learning. *Advances in Neural Information Processing Systems*, 32.
- Michael Saxon, Samridhi Choudhary, Joseph P McKenna, and Athanasios Mouchtaris. 2021. End-to-end spoken language understanding for generalized voice assistants. *Proceedings of Interspeech*.

- Rico Sennrich, Barry Haddow, and Alexandra Birch. 2016. [Neural machine translation of rare words with subword units](#). In *Proceedings of the 54th Annual Meeting of the Association for Computational Linguistics (Volume 1: Long Papers)*, pages 1715–1725, Berlin, Germany. Association for Computational Linguistics.
- Siqi Sun, Zhe Gan, Yuwei Fang, Yu Cheng, Shuohang Wang, and Jingjing Liu. 2020. [Contrastive distillation on intermediate representations for language model compression](#). In *Proceedings of the 2020 Conference on Empirical Methods in Natural Language Processing (EMNLP)*, pages 498–508, Online. Association for Computational Linguistics.
- Yonglong Tian, Dilip Krishnan, and Phillip Isola. 2020. Contrastive representation distillation. *Proceedings of ICLR*.
- Gokhan Tur and Renato De Mori. 2011. *Spoken language understanding: Systems for extracting semantic information from speech*. John Wiley & Sons.
- Jue Wang, Dajie Dong, Lidan Shou, Ke Chen, and Gang Chen. 2023a. Effective continual learning for text classification with lightweight snapshots. In *Proceedings of the AAAI Conference on Artificial Intelligence*, volume 37, pages 10122–10130.
- Liyuan Wang, Xingxing Zhang, Hang Su, and Jun Zhu. 2023b. A comprehensive survey of continual learning: Theory, method and application. *arXiv preprint arXiv:2302.00487*.
- Shipeng Wang, Xiaorong Li, Jian Sun, and Zongben Xu. 2021. Training networks in null space of feature covariance for continual learning. In *Proceedings of the IEEE/CVF conference on Computer Vision and Pattern Recognition*, pages 184–193.
- Yabin Wang, Zhiwu Huang, and Xiaopeng Hong. 2022a. S-prompts learning with pre-trained transformers: An occam’s razor for domain incremental learning. *Advances in Neural Information Processing Systems*, 35:5682–5695.
- Zhen Wang, Liu Liu, Yajing Kong, Jiaxian Guo, and Dacheng Tao. 2022b. Online continual learning with contrastive vision transformer. In *Computer Vision—ECCV 2022: 17th European Conference, Tel Aviv, Israel, October 23–27, 2022, Proceedings, Part XX*, pages 631–650. Springer.
- Zhepei Wang, Cem Subakan, Xilin Jiang, Junkai Wu, Efthymios Tzinis, Mirco Ravanelli, and Paris Smaragdis. 2022c. Learning representations for new sound classes with continual self-supervised learning. *IEEE Signal Processing Letters*, 29:2607–2611.
- Yue Wu, Yinpeng Chen, Lijuan Wang, Yuancheng Ye, Zicheng Liu, Yandong Guo, and Yun Fu. 2019. Large scale incremental learning. In *Proceedings of the IEEE/CVF Conference on Computer Vision and Pattern Recognition*, pages 374–382.
- Mengqi Xue, Haofei Zhang, Jie Song, and Mingli Song. 2022. Meta-attention for vit-backed continual learning. In *Proceedings of the IEEE/CVF Conference on Computer Vision and Pattern Recognition*, pages 150–159.
- Guanglei Yang, Enrico Fini, Dan Xu, Paolo Rota, Mingli Ding, Moin Nabi, Xavier Alameda-Pineda, and Elisa Ricci. 2022a. Uncertainty-aware contrastive distillation for incremental semantic segmentation. *IEEE Transactions on Pattern Analysis and Machine Intelligence*.
- Muqiao Yang, Ian Lane, and Shinji Watanabe. 2022b. Online continual learning of end-to-end speech recognition models. *Proceedings of Interspeech*.
- Rong Ye, Mingxuan Wang, and Lei Li. 2022. [Cross-modal contrastive learning for speech translation](#). In *Proceedings of the 2022 Conference of the North American Chapter of the Association for Computational Linguistics: Human Language Technologies*, pages 5099–5113, Seattle, United States. Association for Computational Linguistics.
- Yuhao Zhang, Hang Jiang, Yasuhide Miura, Christopher D Manning, and Curtis P Langlotz. 2022. Contrastive learning of medical visual representations from paired images and text. In *Machine Learning for Healthcare Conference*, pages 2–25. PMLR.
- Danpei Zhao, Bo Yuan, and Zhenwei Shi. 2023. Inherit with distillation and evolve with contrast: Exploring class incremental semantic segmentation without exemplar memory. *IEEE Transactions on Pattern Analysis and Machine Intelligence*.
- Da-Wei Zhou, Qi-Wei Wang, Zhi-Hong Qi, Han-Jia Ye, De-Chuan Zhan, and Ziwei Liu. 2023. Deep class-incremental learning: A survey. *arXiv preprint arXiv:2302.03648*.
- Hongguang Zhu, Yunchao Wei, Xiaodan Liang, Chunjie Zhang, and Yao Zhao. 2023. Ctp: Towards vision-language continual pretraining via compatible momentum contrast and topology preservation. *Proceedings of ICCV*.
- Yi Zhu, Zexun Wang, Hang Liu, Peiying Wang, Mingchao Feng, Meng Chen, and Xiaodong He. 2022. Cross-modal transfer learning via multi-grained alignment for end-to-end spoken language understanding. *Proceedings of Interspeech 2022*, pages 1131–1135.

A Appendix

A.1 Related Work

A vast array of CL strategies exist in the literature (Wang et al., 2023b; Zhou et al., 2023), which can be categorized into some macro groups: *regularization-based*, *experience replay*, and *architecture-based*. *Regularization* methods contrast

forgetting either by introducing some ad-hoc regularization terms that penalize changes to model weights (Ebrahimi et al., 2020; Kirkpatrick et al., 2017) or to model predictions (Hou et al., 2018; Li and Hoiem, 2017; Fini et al., 2020). *Experience replay* approaches interleave the new data with cherry-picked samples from the prior tasks (Chaudhry et al., 2019; Bang et al., 2021; Buzzega et al., 2020), or they incorporate regularization terms with this additional data to steer the optimization process and prevent catastrophic forgetting (Chaudhry et al., 2019; Wang et al., 2021; Yang et al., 2022b). Finally, *architecture* methods involve creating task-specific/adaptive parameters, such as dedicated parameters to each task (Xue et al., 2022; Wang et al., 2022a) or task-adaptive sub-modules or subnetworks (Aljundi et al., 2017; Ostapenko et al., 2021).

Contrastive learning (Oord et al., 2018; Chen et al., 2020) is a popular approach in self-supervised learning, but it can also be used in supervised learning (Gui et al., 2023) and multi-modal learning (Radford et al., 2021). Its objective is to learn discriminative feature representations by pushing apart different samples (negatives) and bringing closer similar ones (positives). In the case of supervised CIL, it has been shown that endowing the model with contrastive learning objectives results in more robust representations against CF. For incremental semantic segmentation, Yang et al. (2022a) and Zhao et al. (2023) propose to exploit contrastive learning in conjunction with knowledge distillation. For image classification, Wang et al. (2022b) advance a contrastive learning strategy based on the vision transformer architecture for online CL.

A.2 Hyper-parameters

We list the main hyperparameters used for our experiments in table 5. We also mention the number of epochs for each setting. For FSC-3, the number of epochs for each task is {40,30,30}, while for SLURP-3 we use {40,25,25}. For FSC-6 and SLURP-6 we use {40,30,30,30,30,30} and {40,25,20,20,20,20} epochs, respectively. We finally note that we set $lr = 5 \cdot 10^{-4}$ for the text encoder, the ASR decoder and the classifier, while for the audio encoder we set a smaller learning rate, $lr = 5 \cdot 10^{-5}$, because it is pre-trained. For our experiments, we used a single Tesla V100 or Ampere A40 GPU. Finally, each experiment reports the mean and standard deviation over 3 runs for

FSC and 2 runs for SLURP, respectively.

A.3 Additional Details on the Definition of the CIL Setting for SLURP

As the SLURP dataset provides multiple levels of annotations (scenario, action, entity[es]), in principle one could decide to divide the dataset into multiple CIL tasks following one of these criteria. Following (Cappellazzo et al., 2023b), we use the scenarios as splitting criterion because they represent more general concepts than the actions and entities, and then the accuracy is computed on the intent, defined as the pair (scenario,action). In addition to this, we define the order of the classes in the various tasks depending on their cardinality, meaning that the classes with more samples are seen first by the model. This is done because the cardinality of SLURP scenarios varies consistently from class to class, and this should resemble a practical situation in which the model accrues sufficient general knowledge, learning the largest scenarios first, that will be useful for learning more specific scenarios. All in all, we tried to be as consistent with the original implementation in (Cappellazzo et al., 2023b) as possible in order to ensure a fair comparison with prior works.

A.4 SpecAug Details

In this section, we elaborate on the use of SpecAug for augmenting the audio input data. SpecAug (Park et al., 2019) is a popular augmentation technique that is applied directly on the log mel spectrogram of an audio signal, with the aim of making the model invariant to features deformation. In the original paper, they advance three different types of distortions: *time warping*, and *time* and *frequency masking*, where blocks of consecutive time steps and frequency channels are zero-masked, respectively. Since our audio encoders (i.e., DistilHuBERT and Wav2vec 2.0) work on the raw audio waveforms, SpecAug is not applicable by default. In order to circumvent this problem, we apply an approximated version of SpecAug directly to the raw waveform, as proposed in the SpeechBrain library (Ravanelli et al., 2021). We randomly drop chunks of the audio waveform (by zero-masking) and frequency bands (with band-drop filters). Unlike the SpeechBrain implementation, we do not apply speed perturbation. In more detail, with probability 0.5 we randomly drop up to 2 frequencies, while with probability 0.5 we randomly drop up to 3 chunks of audio whose length is sampled from a

Table 5: Training hyperparameters for FSC and SLURP.

Hyperparameter	FSC	SLURP
Batch Size		32
Optimizer		AdamW
β_1		0.9
β_2		0.98
ϵ		10^{-6}
lr		$5 \cdot 10^{-4}$
Weight Decay		0.1
Tokenizer	Word Tok.	BPE Tok.
Beam Search width	5	20
Temperature τ		0.1

Table 6: The accuracy of COCONUT and other methods as a function of the memory size for the SLURP dataset.

Method	Examples per class		
	650	1260	2500
iCaRL	59.94	61.87	63.38
COCONUT	68.08	70.17	71.91
COCONUT + S-KD	70.15	71.41	72.10

uniform distribution $\sim \mathcal{U}(0, 0.05 \cdot \text{len}(x))$, where $\text{len}(x)$ is the length of the considered audio waveform x .

A.5 Additional Results for SLURP

Similar to the study we proposed on the right side of Fig. 4 for the FSC dataset, we here include a similar one for SLURP, where we vary the number of samples per class stored in the rehearsal memory. We report these additional results in Fig. 6. Note that 1260 samples corresponds to 1% of the training data, which is the % we used for our main results. Similar to what we obtained for the FSC dataset, we see that, as we increase the number of retained samples to 2500, the gain brought by COCONUT and its combination with S-KD is a bit smaller but still significant, and this happens because the iCaRL method becomes a stronger and stronger baseline as we increase the % of data. Also, we notice that adding the S-KD approach is more beneficial when we have fewer samples in the memory since the task is way more challenging.

A.6 Computational Time Analysis

In this section, we study the computational cost of COCONUT and compare it with the other baselines. The computational time includes the training

and inference time, as well as the time needed for selecting the rehearsal samples to store in the memory (the S-KD method also computes the pseudo-labels that will be stored in the memory). The main difference between the baselines (ER iCaRL, A-KD, S-KD) and COCONUT is that the baselines focus on the rehearsal data only, while COCONUT is applied to both the rehearsal data (NSPT loss) and the new data (MM loss), and so COCONUT requires an additional compute time due to the MM loss. Nevertheless, this additional time does not hinder its applicability as it is somewhat limited. Indeed, for the FSC-6 setting, the KD baselines require an additional 3/7 % of computational time with respect to the fine-tuning baseline, while COCONUT requires around 11%. For SLURP-3, the KD baselines require around 8% of additional compute time, whereas COCONUT requires around 35%. Undoubtedly COCONUT requires slightly more running time than the other KD baselines that are only applied to the rehearsal samples, but this overhead is minimal and consequently we believe this is not an issue for a practical scenario, considering also that COCONUT leads to much-improved performance. Additionally, from a memory overhead point of view, COCONUT requires the storage of the rehearsal samples and a copy of the model from the previous task. These storage requirements are the same as the A-KD baseline. Instead, the S-KD approach, in addition to the aforementioned storage requirements, also necessitates the storage of the rehearsal text transcriptions generated with beam search from the previous task, thus increasing the requested memory overhead with respect to COCONUT.

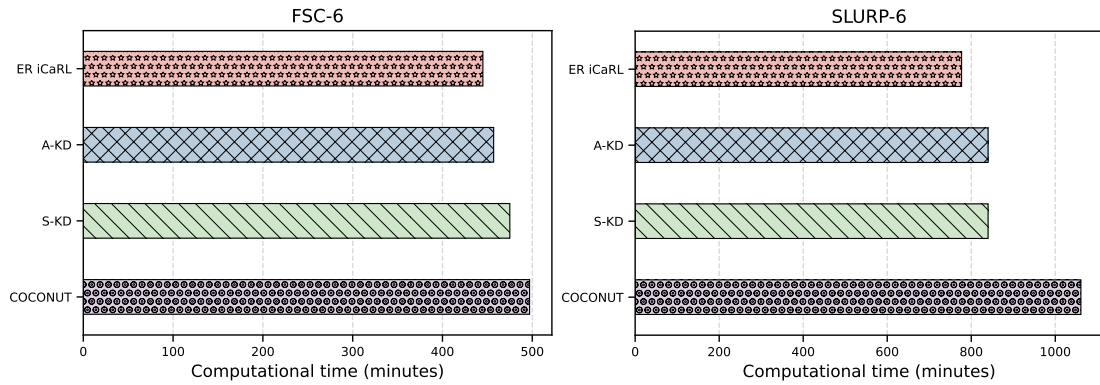


Figure 5: Computational cost analysis of various CIL methods for FSC-6 (*left*) and SLURP-6 (*right*).

A.7 Future Work

COCONUT relies on two contrastive learning-based losses applied to the projections of audio and text encoders outputs. In principle, COCONUT could be exploited in other multi-modal settings such as audio-vision or vision-language. Therefore, it would be interesting to study whether COCONUT can be exploited in other different multi-modal scenarios. Also, since these settings usually involve a larger number of classes than ours, we would be able to test how COCONUT scales to the number of tasks.